NUCLEAR INSTRUMENTS AND METHODS 130 (1975) 507–511; © NORTH-HOLLAND PUBLISHING CO.

A MULTI-ELEMENT LEAD GLASS CHERENKOV DETECTOR

CH. BERGER, R. BÜHRING, G. DICK, W. ERLEWEIN*, R. GRIGULL, N. MISTRY† and D. TRINES

I. Physikalisches Institut, RWTH Aachen, Aachen, Germany

Received 19 September 1975

A detector is described which was designed for the detection of photon pairs from the decay of π^0 mesons following an electroproduction experiment.

The detector consists of a large number (at present 182) of single Cherenkov counter modules and has a γ-detection efficiency of practically 100%.

1. Introduction

The detector described here was designed to detect photon pairs from the decay of π^0 mesons in an electroproduction experiment of the type

$$e+p \rightarrow e+\pi^0+X.$$

Due to the much reduced flux of incoming virtual photons compared to a typical photoproduction experiment a hodoscope consisting of spatially separated elements, as had been used in previous experiments[1]), seemed to be bad, acceptance-wise. In the planned experiment[2]) the available solid angle is essentially determined by a large gap sweeping magnet and is in the order of 50 msr. In order not to loose any detection efficiency for γ quanta the whole available solid angle has to be covered by a photon detector, e.g. a lead glass wall of 1 m² area at a distance d of typically 4.50 m to the target. If the π^0 meson is to be defined by the invariant mass $m_{\gamma\gamma}$ of the decay photons

$$m_{\gamma\gamma}^2 = 4k_1 k_2 \sin^2 \alpha, \tag{1}$$

the energies k_1, k_2 and the positions (which define the opening angle 2α) have to be measured separately. Therefore the counter consists of a large number (at present 182) of single Cherenkov counter modules, which determine energy and position of the incoming γ quanta. The further advantage of such a system in comparison to a detector using converters and wire planes is, that the detection efficiency of γ quanta hitting the wall is practically 100%. Beside the very good π^0 definition this modular set-up can be widely used in any multi-γ-ray experiment.

2. Description of a module

The size of the modules is given by the mass resolution wanted:

$$\frac{dm_\pi}{m_\pi} = \left(\frac{1}{4}\left(\frac{dk_1}{k_1}\right)^2 + \frac{1}{4}\left(\frac{dk_2}{k_2}\right)^2 + \left(\frac{d\alpha}{\alpha}\right)^2\right)^{\frac{1}{2}}. \tag{2}$$

Assuming symmetric decay of the π^0 one has $m_\pi \approx E_\pi \alpha$, $k_1 = k_2 = \frac{1}{2}E_\pi$, which results in a required spatial resolution of

$$\Delta X = \frac{\Delta k}{k}\frac{m_\pi}{E_\pi} d, \tag{3}$$

for *equal* contribution of spatial and energy resolutions of a module.

With lead glass the achievable energy resolution is typically $(\Delta k/k)_{\text{rms}} = 0.07/\sqrt{(K[\text{GeV}])}$ which gives $\Delta X \approx 20$ mm at $E_\pi = 2$ GeV. If all the energy is contained in one block of sidelength a, the spatial resolution is given by $\sigma = \frac{1}{2}a/\sqrt{3}$ which results in $a = 65$ mm. In addition this size allows the use of cheap standard 2″ tubes.

The uncertainty in the energy determination of incoming photons or electrons is mainly coming from two sources.

a) The shower leakage through the lead glass block. The shower development in cylindrical blocks of given length and diameter has been calculated by several authors using Monte Carlo techniques[3]). In fig. 1 the fraction $f = E/E_0$ of the absorbed energy in a lead cylinder is plotted versus the length in units of the radiation length X_0. Nagel[3]) estimates that the contribution to the line width, due to the fluctuation of f is given by

$$\left(\frac{\Delta E}{E_0}\right)^2_{\text{shower, rms}} = \frac{10(1-f)}{E_0}; \tag{4}$$

E_0 in MeV.

* Present address: Messerschmidt-Bölkow GmbH, Munich, Germany.

† Present address: Cornell University, Ithaca, N.Y., U.S.A.

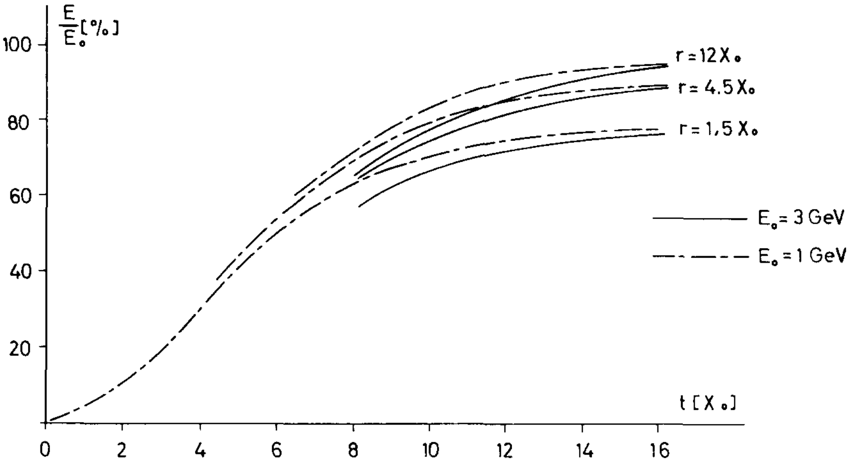

Fig. 1. The percentage of primary energy which is absorbed in a lead cylinder of radius r and length t (ref. 3).

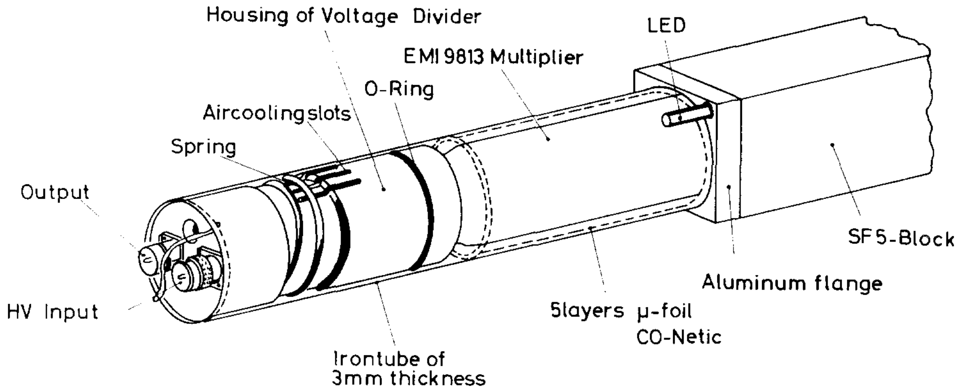

Fig. 2. Schematic drawing of a counter module.

b) Photoelectron statistics. Knowing the number $\pi(E_0, t)$ of shower electrons at a depth t of the block, the spectrum $C(\lambda)$ of the Cherenkov light, the transmission $D(t, \lambda)$ of the glass, the quamtum-efficiency of the photocathode $Q(\lambda)$ and the fraction ζ of light which hits the photocathode, one can calculate the number of photoelectrons

$$N_p = \xi \int_0^{t_0} dt \int \pi(E_0, t) D(t, \lambda) Q(\lambda) C(\lambda) d\lambda, \qquad (5)$$

with

$$C(\lambda) = \frac{2\pi}{137}\left(1 - \frac{1}{\beta^2 n^2}\right)\frac{1}{\lambda^2}.$$

To an approximation, which is good for estimates, ζ is given by the ratio of the area of the photocathode to the area of the block surface.

The contribution of photon statistics to the total line width is then given by

$$\left(\frac{\Delta E}{E}\right)^2_{\text{phot, rms}} = \frac{1}{N_p}\frac{v_i}{v_i - 1},$$

where v_i is the phototube amplification per dynode. Calculating the expected total line width

$$\left(\frac{\Delta E}{E_0}\right)^2_{\text{tot}} = \left(\frac{\Delta E}{E_0}\right)^2_{\text{shower}} + \left(\frac{\Delta E}{E_0}\right)^2_{\text{phot}}, \qquad (6)$$

we found a shallow minimum for a block length between $12X_0$ and $15X_0$, and chose the length to be $12X_0$. The minimum arises from the fact that increasing the length of the glass block decreases the contribution of shower statistics, but also decreases the number of photoelectrons because of the finite transmission of the lead glass.

In order to keep ζ large it is important to closely match the cross section of the block face to the diameter of the phototube.

For practical reasons (easy replacement of tubes, easy pile-up of the wall in different shapes) we wanted the phototube with base and housing and the lead glass block to form a single module. Such a module is shown in fig. 2.

An aluminum flange is glued to the SF 5 glass block (dimension $64 \times 64 \times 300\ mm^3$). The glass block is wrapped with a 0.02 mm aluminum foil and for mechanical protection packed in a 0.7 mm shrink tube. The phototube housing consists of an iron tube (wall thickness 3 mm), which is glued on to the aluminum flange. The phototube (EMI 9813) is pressed on the glass block by a strong spring. The optical contact is achieved by a 2 mm layer of silicone rubber (Silopren, Bayer–Leverkusen). The voltage divider has very small dimensions, mainly due to using zener diodes across the last dynodes instead of large capacitors.

3. Calibration of the detector

All 182 elements have been carefully tested and calibrated in an electron test beam at DESY. The beam spot ($5 \times 5\ mm^2$) on the glass block was defined by two crossed finger counters S1 and S2. Coincidence of S1 and S2 together with a further downstream scintillation counter S3 opened the gate of a 256-channel ADC (Nuclear Enterprise Octal ADC 9040) which was then read out by a PDP 11/10 computer. The energy spread of the electron beam was about $\sigma = 1.3\%$. Spectra have been taken at electron energy E from 0.5 to 4 GeV in steps of 0.5 GeV, with the beam hitting the center of the block. In fig. 3 the measured averaged pulse height is plotted versus the beam energy for a typical element. The response is very linear.

A typical pulse height distribution for $E_0 = 1$ GeV is shown in fig. 4. From this curve we deduce an energy resolution of $(\Delta E/E_0)_{rms} = 7\%$ at 1 GeV. Fig. 5 shows

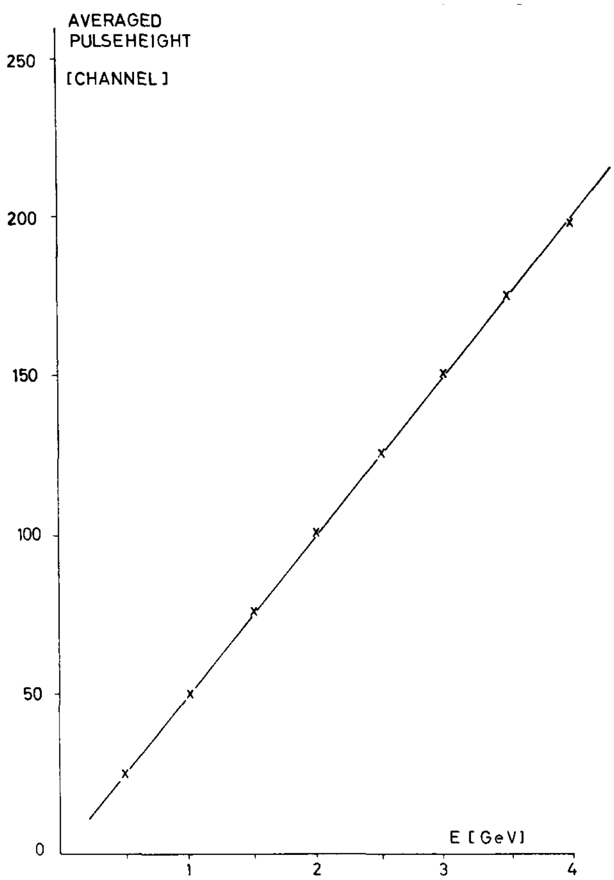

Fig. 3. The energy calibration. Averaged pulse height vs electron energy E_0.

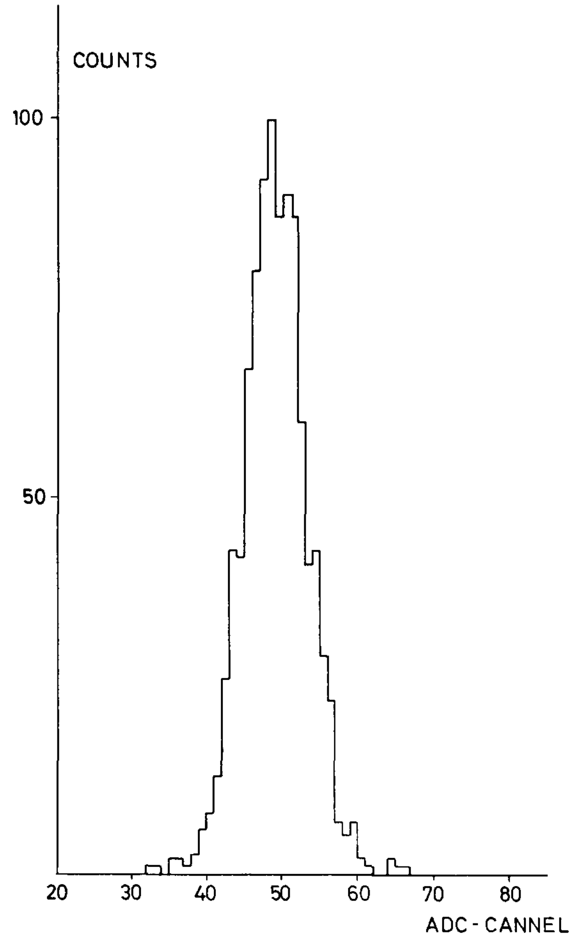

Fig. 4. The pulse height distribution for 1 GeV electrons. Counts vs pulse height.

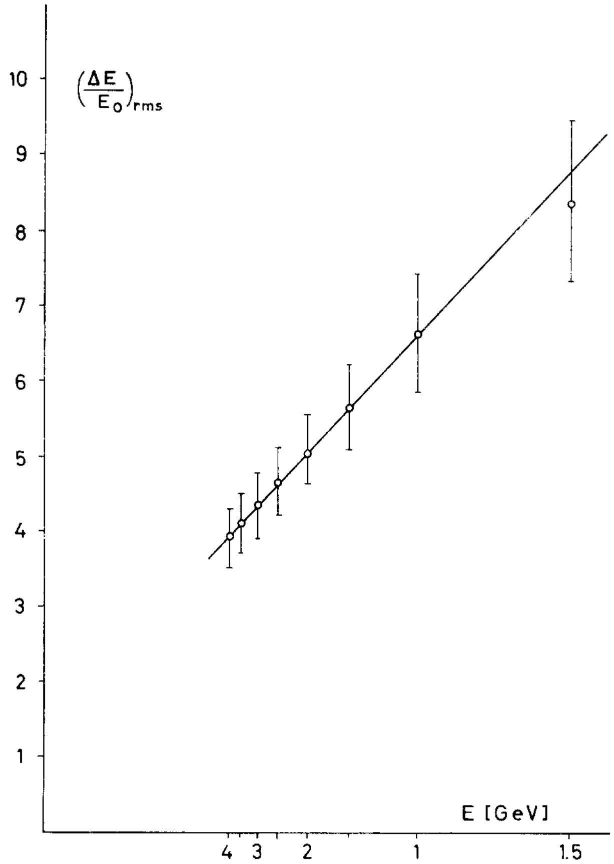

Fig. 5. The averaged energy resolution of all 182 elements vs $1/\sqrt{E_0}$. The bars indicate the spread of resolution among the 182 modules.

the energy resolution averaged over all 182 elements plotted versus $1/\sqrt{E}$. The straight line follows a $1/\sqrt{E}$ law between E = 0.5 and 4 GeV. The separate contribution of shower statistics and photon statistics can be calculated from eqs. (5) and (6).

For $E = 1$ GeV we get

$$\left(\frac{\Delta E}{E_0}\right)_{\text{shower}} = 5.1\,\%; \qquad \left(\frac{\Delta E}{E_0}\right)_{\text{phot}} = 4.3\,\%.$$

With the beam on the center of the glass block about 10% of the light is shared between the 8 neighbouring blocks. In principle one would expect an improvement of the resolution by adding the pulse heights of these blocks to the central blocks. In practice this is not the case, mainly because of bias fluctuation of the ADCs (1 to 2 channels).

In fig. 6 the averaged pulse height of one block is plotted versus the beam position on the glass face for $E = 1$ GeV. Within $\Delta X = \pm 15$ mm the pulse height does not drop by more than 5%.

The peak value of the summed total pulse heights of neighbouring modules did not change by more than 2% when we scanned with a 5×5 mm^2 beam across the border of two adjacent blocks.

Due to the fact that most of the shower energy is contained in a relatively small cylinder with a radius of about 20 mm (fig. 1) the spatial resolution is essentially determined by the chosen block size. At least near the edge of the block the spatial resolution can be improved considerably by taking into account the amount of energy shared between different blocks.

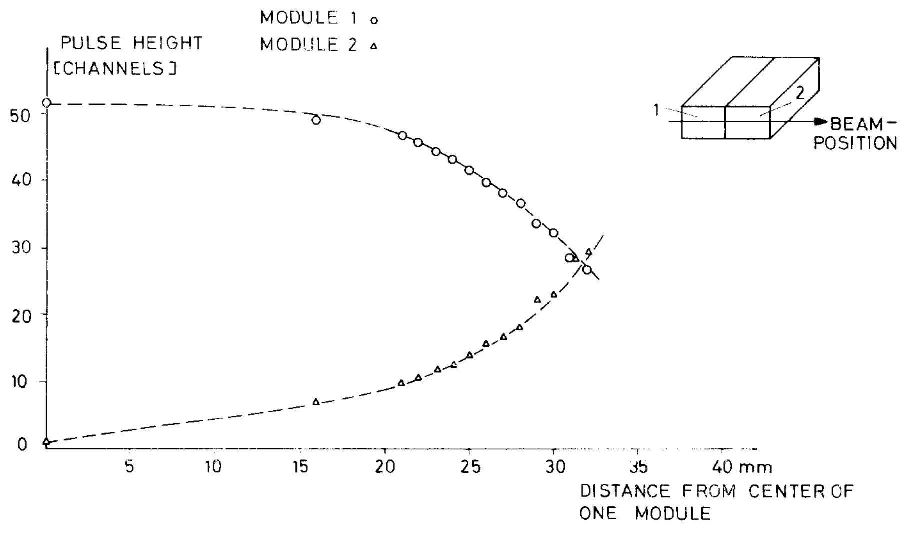

Fig. 6. The averaged pulse height of one module vs the beam position on the glass face for 1 GeV.

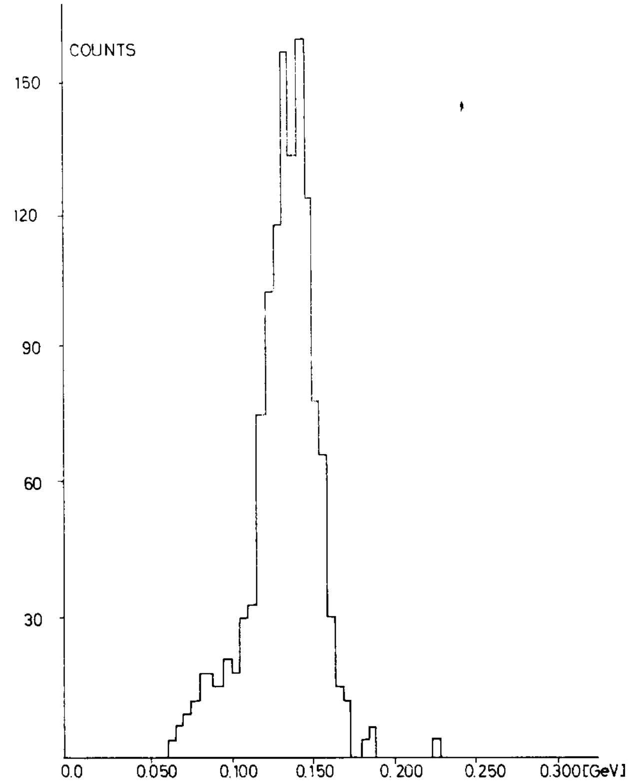

Fig. 7. The invariant mass plot of $\gamma\gamma$ events in the reaction $e+p \to e+\pi^0+X$.

Furthermore we checked the response of the detector to electrons which do not hit the block face perpendicularly. For deviations from perpendicular incidence up to 15° the pulse height drops by less than 3%.

4. Stability

In order to control the gain of the phototubes each element is equipped with a LED (MV 52 Monsanto) mounted at the *rear* end of the glass block (fig. 2) for practical reasons only. All the LEDs are driven by one precision pulser followed by a 200-fold active fan-out. The LEDs are fired between beam spills of the synchrotron. Each diode was set individually during the calibration runs in order to give a response around channel 100 of the ADCs.

By comparing the results of different calibration runs we found that LEDs are a very good light normal provided one accounts for the temperature dependence in the light output, which we measured to be 0.5% per degree in our range of interest. The stability of the LED pulser and the gain of the ADCs is continuously checked during the experiment. If the gain of the phototubes changes due to ageing, varying beam load or influence of magnetic fields e.g., we change the PM high voltage until the LED signal is back to its nominal value. This is done during the experiment by an automized system. The computer compares the output of the LED continuously with a list of nominal values stored in the memory. The high voltage is changed via individual step motors connected to each potentiometer in the high voltage divider system. This system will be described in detail in a further publication.

5. π^0 detection

In order to detect π^0 mesons 4 blocks are defined to be a cell. In the logic part of the electronics the sum output of a cell is connected to a discriminator. If the energy deposit in a cell is higher than a given threshold, the discriminator fires. If 2 or more *cell* discriminators are set, the gates of the ADCs are opened and the energy deposit in each *block* is recorded.

Fig. 7 shows a plot of the $m_{\gamma\gamma}$ invariant mass obtained in the experiment mentioned earlier. The mass resolution is $\sigma = 15$ MeV and compares very well with Monte Carlo calculations.

The authors wish gratefully to acknowledge the constant support of Prof. L. Lübelsmeyer. We would like to thank Prof. D. Schmitz for many discussions. We thank the DESY Direktorium for their kind hospitality and the DESY Hallendienst for their friendly help. We appreciate very much the invaluable work of our technician H. Vennemann.

References

1) Ch. Berger, G. Dick, W. Erlewein, K. Lübelsmeyer, L. Paul, H. Meyer-Wachsmuth and A. Schultz von Dratzig, Phys. Lett. **47B** (1973) 377.

2) H. Ackermann, T. Azemoon, Ch. Berger, G. Dick, E. Ganßauge, F. Janata, D. Lücke, D. Schmidt, G. Specht and D. Trines, DESY – Proposal 125 (1973).

3) For 1 GeV data see: H. Nagel, Z. Physik **186** (1965) 319; for 3 GeV data see: H. Burfeindt, DESY 67/24.